

**STOCHASTIC MODELING OF THE QUORUM
SENSING NETWORK IN *AGROBACTERIUM*
*TUMEFACIENS***

A Senior Thesis
Submitted to the
Department of Biology,
The Colorado College

By
Brendan Davis

Date _____

Approved by:

Primary Thesis Advisor

Secondary Thesis Advisor

Brendan Davis 2015
Colorado College
Spring 2015

Stochastic Modeling of the Quorum Sensing Network in

Agrobacterium Tumefaciens

Abstract

Stochastic Modeling of the Quorum Sensing Network in *Agrobacterium*

tumefaciens Brendan Davis*, Leigh Nicholl, David Brown, and Phoebe Lostroh,

Departments of Mathematics and Biology

For years, prokaryotes were thought to be simple, single cell organisms without communicate or interact. We now know bacteria, such as *Agrobacterium tumefaciens*, use small, autoinducing molecules to sense population densities. This “quorum sensing” (QS) model works on a positive feedback loop and signals the bacteria to insert a tumor inducing (Ti) plasmid into the nucleus of a plant cell by horizontal gene transfer. Here, we used a stochastic model to mathematically evaluate the quorum sensing system. We found under certain conditions the model acted as a “bistable switch”, turning the system “on” and “off” at random. When a second cell was introduced to the model it increased the probability of the system turning “on”. We also found that by manipulating various variables we could alter the frequency of the QS network turning “on”. With this research, we are able to better understand the coordination involved in the infection of host plants by *Agrobacterium tumefaciens*. Thus, we can predict possible treatments for the progression of tumors in plants that are infected by crown gall disease. This type of model has implications to many other mathematical models in which this “bistable” phenomenon may be observed, as well as applications to other quorum sensing networks.

Introduction

Gram-negative and Gram-positive Bacteria

A large majority of the living organisms around us are microscopic organisms that can't be seen with the naked eye (Schaechter, Ingraham, & Neidhardt 2006, p.3). The study of these *microbes* has become increasingly significant because of their overwhelming existence – far greater in number than the organisms we can actually see. All microbes can be classified into one of two categories: prokaryotes and eukaryotes (Schaechter, Ingraham, & Neidhardt 2006, p. 3). What differentiates the two types of microbes is the presence of a true nucleus. Eukaryotes pack DNA into a membrane-bound nucleus where as prokaryotes do not. In fact, prokaryotes do not have membrane-bound organelles, such as mitochondria and chloroplasts, as well. Because of this distinction, prokaryotic organisms have a thick cell wall made up of short glycan chains cross-linked by peptides, called peptidoglycan, to protect from inside and outside pressures (Sauvage et al., 2008). Murein is a particular type of peptidoglycan specific to bacteria (Schaechter, Ingraham, & Neidhardt 2006, p. 24). This structure is also responsible for the shape and structure of the cell itself. The constituents that make up a cell wall may also cause the death of a prokaryote by a host's immune system. Commonly known as microbe-associated molecular patterns (MAMPs), these antigen specific targets help distinguish healthy human cells against foreign bacterial invaders, so a proper immune response can be elicited (Schaechter, Ingraham, & Neidhardt 2006, p.408-411). Because it is so important to prokaryotic cell survival, peptidoglycan may also be a target for many antibiotic drugs (Schaechter, Ingraham, & Neidhardt 2006, p. 24). Different Bacteria have

structural modifications in the surrounding cell envelope in an attempt to protect against these pressures (Schaechter, Ingraham, & Neidhardt 2006, p. 22).

Bacterial prokaryotes can be subdivided into two groups based on their overall pattern of this outer envelope structure. A form of staining is used to differentiate gram-positive and gram-negative bacteria by dyeing the former purple and the latter red (Schaechter, Ingraham, & Neidhardt 2006, p.23). This Gram stain, named after the Danish microbiologist who developed it, is the result of fundamental differences in the structure of the cellular envelope. In comparison to gram-positive bacteria, gram-negative bacteria have a much thinner cell wall, which is sandwiched between an inner and outer cell membrane made of a phospholipid bilayer (Figure 1). Conversely, gram-positive bacteria lack an outer membrane, and thus have a much thicker cell wall (Figure 1). With the varying structures that make up these cell envelopes, the ability for each type of bacteria to secrete and allow diffusion of molecules into the cell will vary as well (Miller & Bassler, 2001). Here, I will focus on the secretion of a small, signaling molecule used to regulate gene expression for a population of bacteria.

Quorum Sensing

Many cells, prokaryotic and eukaryotic alike, use signaling to communicate among each other and control the expression of genes. Your own immune system uses small soluble proteins, known as cytokines, to communicate between the cells of the immune system and coordinate an effective immune response against foreign pathogens (Parham, 2015, p.53). Until recently, bacteria were thought to exist as individual cells without the ability to interact with surrounding cells (Miller &

Bassler, 2001). The exchange of molecules between cells was thought to be characteristic of only eukaryotes. However, scientists have recently discovered that bacteria have the ability to signal other cells to coordinate physiological activity as a population – called quorum sensing. This phenomenon was first described in *Vibrio fischeri* over forty years ago (Nealson & Hastings, 1979). A symbiotic relationship between *Euprymna scolopes* (Hawaiian bobtail squid) and *V. fischeri* allows the squid to camouflage itself – utilizing the quorum sensing network of the bacteria, which feed off the nutrient rich environment of the squid. *E. scolopes* collects the bacteria throughout the day in a complex light organ within the mantle cavity on its body. When the bacteria reach a population density threshold (quorum), they coordinate the expression of a bioluminescent gene to light up the underside of the squid (Miller & Bassler, 2001). The squid uses the light as counterillumination to camouflage itself from predators. Since the discovery of quorum sensing, this form of cell signaling to sense a population has been described in a wide range of organisms. Many pathogens use quorum sensing to regulate the expression of virulence genes that are important to the infection process. For instance, methicillin-resistant *Staphylococcus aureus* (MRSA), a deadly, antibiotic-resistant pathogen, uses quorum sensing to upregulate the expression of adhesion molecules to form a biofilm – a necessary component of infecting its host (Rutherford & Bassler, 2012). *Agrobacterium tumefaciens* utilizes quorum sensing to control the horizontal gene transfer of a tumor inducing plasmid into its host plant cell in order to cause crown gall disease (Haudecoeur & Faure, 2010). Quorum sensing is important to the survival of many species of bacteria. By using small, diffusible molecules known as

autoinducers bacteria can act as a group to benefit from the population-wide coordination of gene expression that regulates various physiological factors.

Autoinducers are small molecules that can be diffused in and out of cells to regulate gene expression of itself and other physiological adaptation genes (Wilson et al., 2011, p. 292). In this way, quorum sensing works on a positive regulatory feedback control loop, but for the system to turn on autoinducer molecules must be constitutively expressed at low levels or else the quorum sensing system would not work. However in some cases, regulation of the autoinducer may also be controlled by an outside source as with *Agrobacterium tumefaciens* (Goryachev et al., 2005). Because of the differences in cell structure between gram-positive and gram-negative bacteria, there are different types of autoinducers that are secreted for each (Miller & Bassler, 2001). The former uses peptide-mediated quorum sensing to sense cell population density. In this way, gram-positive bacteria secrete small autoinducing peptides (AIPs) across the cell envelope to signal other cells in close proximity. In comparison, gram-negative bacteria secrete small, hydrophobic homoserine lactone molecules (HSL) that are freely diffusible across the cell membrane – it can be transported across without the help of a pump or channel. This characteristic is essential to understanding the behavior of a quorum sensing network because it causes equal concentrations of the autoinducer both inside and outside a single cell. However, some cells may be able to create a concentration gradient by actively transporting the autoinducer across the cell membrane in one direction (Goryachev et al., 2005). At low levels of constitutive expression, the autoinducer will diffuse into the extracellular matrix and be lost or degraded, thus

not affecting the expression of target genes. However, when enough bacteria accumulate the concentration of autoinducer reaches a threshold that allows the population to turn “on” specific genes. This phenomenon can be modeled using differential equations to understand the conditions necessary for a bacterium to turn “on”. In this paper, I model the quorum sensing network of *Agrobacterium tumefaciens*.

Agrobacterium is a genus of bacteria responsible for the infection of a wide range of plants (Goryachev et al., 2005). Of these, the soil bacterium *Agrobacterium tumefaciens* is the most extensively studied. A gram-negative bacterium, *A. tumefaciens* utilizes quorum sensing to cause tumors in various species of plants (Haudecoeur & Fauer, 2010). The bacterium can sense plant wounds, which it feeds on, by using chemotaxis to recognize exudates secreted from the wound (Goryachev et al., 2005). Upon recognition of an injured plant, the bacterium attaches itself to the root and activates its virulence genes to induce the horizontal gene transfer of a tumor inducing (Ti) plasmid into the host plant cell. The plasmid is incorporated into the plant cell’s genome to cause overexpression of growth factors from oncogenes (Gohlke & Deeken, 2014). Gall tumors resulting from vigorous proliferation are the characteristic signs of crown-gall disease in plants caused by *A. tumefaciens*. The Ti plasmid not only encodes for the oncogenes that cause the tumor, but it also stimulates the plant to synthesize opines for the bacterium to feed off of (Goryachev et al., 2005). These opines help to activate the quorum sensing system in *A. tumefaciens* to cause a population wide infection of the host plant. The autoinducer of the bacteria, 3-oxo-octanoyl homoserine lactone (OC8HSL), further

promotes the conjugation of the Ti plasmid by up to eight-fold (Subramoni et al., 2014). This quorum sensing network is necessary to establish a rapid and efficient infection against the plant host, as well as limit conjugation by a single cell as it is an energy consuming process and it would not be able to elicit a proper infection of the host plant. A proposed model by Andrew B Goryachev et al. (2005), simulates the regulation of the complex network (Figure 2). We examine this network in our own model (Figure 3) to examine the differences between a deterministic model (Figure 4A) and a stochastic model (Figure 4B-D). By adapting Goryachev et al.'s model to a two-cell model (Figure 5) and predicting various rates, we use stochastic mathematical modeling to predict the probability of the bacterium turning "on" in the presence of its autoinducer.

Mathematical Modeling

Until recently, mathematicians and biologists have been separated by a lack of overlapping interest in the two fields. Biologists could have cared less about differential equations, and likewise mathematicians refrained from studying the interworking machinery of a cell that regulates gene expression. However, mathematical biologists have learned to mesh the two fields together in order to better understand the world around us. Mathematical models have a wide range of application for biological systems. They can be used to predict the spread of swine flu during the 2009 pandemic (Al Hajjar & McIntosh, 2010), examine the progression of cancer cells (Gentry & Jackson, 2013), or even track the population dynamics of a complex microbial ecosystem (Haruta et al., 2013). Variables can be

manipulated and the effects observed to, for example, see the effectiveness vaccination might have during the H1N1 outbreak (Al Hajjar & McIntosh, 2010).

Most mathematical models do a fairly good job at estimating what may happen in a given system; however, few take into account the variability that may occur with any real-life biological system. Stochastic models allow a certain amount of variation to leak into the model. At each time step, the model is reevaluated for the next time step based on probability (Wilkinson, 2012, p. 3-20). This differs from a deterministic model in which the results are entirely determinate on the variables you feed the model. This, of course, is not accurate to a real life biological system in which variability plays a huge role. You may wonder why more models don't employ stochastic variation to simulate their biological system. This is because stochastic models, when run on a computer, can be very time consuming especially when manipulating a whole range of variables. Deterministic models are therefore used when minute details do not matter as much and you are more interested in looking at the whole picture. With differential equations as the structure of our model, we use stochasticity to make the system non-deterministic. This particular method is especially important for our model, in which we care about the slight variations in autoinducer density. These small variations may determine whether or not the quorum sensing system turned "on" during a set time frame. With a stochastic approach we can be more confident that our model is accurate to the quorum-sensing regulation in *A. tumefaciens*.

In this paper, we use a set of differential equations to predict the "on"/"off" switch of the quorum sensing network in *A. tumefaciens*. The differential equations

are produced by the input of a series of simple biochemical reactions that take place as part of the large quorum sensing network. Most mathematical models of quorum sensing use either a single-cell model or a large population wide network of cells (Goryachev et al., 2005). However, we hypothesize more information can be obtained when using a two-cell model. At first we examine the characteristics of a single-cell model (Figure 3) to better understand our two-cell model (Figure 5). We used the basic single-cell structure of Goryachev et al.'s model (2005) to create a model in which two cells are communicating back and forth by the means of an autoinducer (Figure 5). By including rates of cell exchange and autoinducer turnover we can manipulate these variables to examine the effects each has on the overall network. We found that increasing the rate of these variables correlated with an increase in the probability of the quorum sensing system turning "on" over time.

Results

While manipulating different variables in the single-cell model, we noticed an interesting phenomenon: the stochastic model behaved in such a way that it could turn "on" and "off" spontaneously when looking at the variable of interest, TraRdim. When compared to the deterministic model (Figure 4A), the stochastic models (Figure 4B-D) seemed to have a level of randomness that could flip the system back and forth between these two states. Essentially, the model had become "bistable" under certain conditions. This meant that the model could exist in two different states – "on" and "off" and it could spontaneously switch between these states, remaining in one or the other for a seemingly random amount of time. This

“bistable” behavior held true for multiple runs of the model. We were curious to see what sort of variables may cause the system to turn “on” more frequently or which ones could stop the quorum sensing network from ever turning on in the first place. With this information, we moved to a two-cell model to observe the interacting behavior between two bacteria.

For the two-cell model, we were curious in the effects of two specific variables, which linked cells together in a quorum sensing model: cell exchange rate and turnover rate. Each bacteria could be either “on” or “off” which was determined by the level of TraRdim within each cell. As with the single-cell model, if the population of this dimer exceeded 100 particles, the system was determined to be “on”. If cells agreed with each other – both turned “on” (Figure 4B) or both remained “off” (Figure 4C) – the bacteria were ‘synchronized’. However, if the cells behaved differently over the 10,000-second time course they were independent and therefore not synchronized (Figure 4D). The ‘probability of synchronization’ increased with an increase in both cell exchange rate and turnover rate (Figure 6). At a low exchange rate, of one AAI particle per second, the amount of synchronization steadily increased between 20% and 100% with an increase in turnover rate. Though it eventually reached 100%, it should be noted all values of cell exchange rate had 100% synchronization when the turnover rate was at its highest. At a cell exchange rate of three particles per second, the cells synchronized more, ranging from 50% to 100%. The only drop off from a steady increase at this value of cell exchange occurred between a turnover rate increase from 0.03 to 0.04 in which the synchronization dropped from 80% down to 70%. For a high cell

exchange rate of five particles per second, the cells synchronized even more so, ranging from a minimum of 70% up to 100% with a steady increase.

A similar method was used to examine the likelihood of a cell turning “on”. If the amount of TraRdim exceeded 100 particles for either cell in the time course it was tallied as “on”. Cells had a higher ‘probability of “on”’ with an increase in both cell exchange rate and turnover rate, adjusted independently (Figure 7). As with synchronization, the probability of turning “on” reached 100% at the fastest turnover rate for all cell exchange rates. At an exchange rate of one particle per second, the probability of a cell turning “on” steadily increased from 50% to 100%. With the cell exchange rate set to three particles per second the probability ranged between 55% and 100%. At the highest exchange rate of five particles per second, the range fell between 65% and 100%. For each cell exchange rate, the probabilities of turning “on” all increased steadily in their noted ranges as turnover rate increased.

Discussion

Our stochastic models (Figure 4B-D) behaved drastically different than the deterministic time course (Figure 4A) under the conditions of Goryachev et al.’s 2005 model (Table 1). Because of the “bistability” our model produced, we know precise conditions must be at play for the quorum sensing system to turn “on”, and consequently induce the transfer of the Ti plasmid to the host plant by horizontal gene transfer. Without these conditions, *Agrobacterium Tumefaciens* would be unsuccessful at infecting its host plant with crown gall disease. This phenomenon is rather interesting in the realm of mathematical biology as most stochastic models

behave in close coordination with its deterministic counterpart. A stochastic model may perhaps leap away from the deterministic trend at times, but usually find its way back shortly after.

Goryachev et al. found the model behaves more closely to the deterministic model with a growing population (2005). This means the system becomes less random at high densities of bacteria. However, we were curious if the quorum sensing system could still work in an intermediate stage where population densities are lower and the system becomes more random. In fact, we looked at the dynamics between two single cells. We found under certain conditions, *Agrobacterium tumefaciens* may actually be able to coordinate infection of a host plant cell at a low population. This becomes increasingly true as the bacteria communicate at a faster rate or there is a faster turnover of the autoinducer through the outside medium. It may be apparent that if two cells are communicating better than they can coordinate physiological activity better. However, it is somewhat unclear why an increase in turnover rate may cause similar effects. The turnover rate is somewhat like a hose spraying autoinducer past the cells at a certain rate. As you increase the rate of flow from this hose, you would theoretically make it more difficult for any autoinducer released from a cell to be diffused back into another cell. This was not the case for our model in which an increase in turnover rate caused an increase in both cell synchronization (Figure 6) and the probability of a cell turning “on” (Figure 7). An increase in both of these increases the power of the quorum sensing network to elicit the transfer of a tumor inducing plasmid into the host plant. This may be a result of our model and *rate law for AAI supply* which takes into account many

variables; however, I believe the quorum sensing network may actually be more effective with an increase in turnover rate. This essentially brings in more autoinducing signal from other cells outside of the system so the cells can communicate better. This does not alter the density of this signal outside the cell at any given time, but rather changes the rate at which it is replaced. With this theory, we can begin to think of possible treatments for crown gall disease by slowing down or possibly stopping the quorum sensing in *A. tumefaciens*.

A second cell seemed to increase the probability of the quorum sensing system turning on, especially when the cells were communicating at a faster rate or when the turnover rate was high. In real life application, cell exchange rate can increase because of the medium in which the bacteria are or because of the distance between the two cells. Turnover rate may also be affected by the medium, as diffusion may occur quicker in a less dense environment or vice versa. As more cells accumulate, the turnover rate is likely to increase as well for a given cell, thus increasing the likelihood of the system turning “on”. This is the phenomenon of quorum sensing!

Because our variables were estimates of the actual rates for cell exchange and turnover, our model may be inaccurate to the real life quorum sensing network of *A. tumefaciens*. Further investigation would be necessary to discover the actual rates in a wet lab. We could employ these rates to our model to better understand the coordination of the bacteria to infect its host plant. However, our estimates give insight into the effects these rates may have on the overall network. The trends we

observed could be realistic to the system unless the actual rates are vastly different than our estimations predict.

In the realm of biology, this research is vital to the understanding of the progression of crown gall disease by *A. tumefaciens*. Because some of the variables we looked at were estimated without any actual raw data, we could measure these values experimentally in a lab to better grasp the true application of our model to the bacterium. However, we know the effect these variables can have on the quorum sensing system to possibly find cures for crown gall disease. Using this model, we can continue to assess the different variables that may increase or decrease the likelihood of the quorum sensing system turning “on”. With this knowledge, we may be able to disrupt one of the factors vital to quorum sensing to prevent the conjugation of the Ti plasmid into a host cell. This is perhaps an effective way of fighting crown gall disease in many species of plants infected by *A. tumefaciens*. One possible treatment as a result of this research may be to coat the gall of an infected plant in a thick, viscous liquid that may perhaps slow the progress of quorum sensing by decreasing the turnover rate of the autoinducer. We could add this variable to our model to observe the possibilities a treatment may have on the model.

Materials and Methods

Quorum Sensing Model

The single-cell model (Figure 3) implemented in this research is based on Goryachev et al.’s complex model (Figure 2). All rates of biochemical processes are recorded in Table 1. These rates are mostly based from Goryachev et al.’s 2005

paper and are for the most part referenced from other research done in labs. In this model, the agrobacterium autoinducer (AAI) can diffuse in and out of the cell freely or be actively transported across the cell membrane by an importer protein (Imp). Octopine molecules (oct) in the environment are metabolized by the bacterium, which promotes the transcription of the *occ* operon at a maximal rate. This operon transcribes the importer mRNA (*imp*) and a *traR* mRNA needed for activation of quorum sensing transcription. If AAI is not present within the cell, *traR* is further translated into a misfolded protein and degraded. However, if AAI is available, TraR forms a tight complex with the autoinducer as it is translated. Once bound to its cognate autoinducer, TraR will not dissociate. Instead, this complex pairs with another to form TraRdim, a dimer that activates transcription, and subsequently translation, of many proteins necessary for conjugation of the Ti plasmid. The dimer itself is not as stable as the complex formed prior, and therefore may dissociate at a given rate. One operon regulated by TraRdim is the *trb* operon, which codes for an enzyme necessary to create AAI. TraI, an acyl-homoserine lactone synthetase, uses two proteins found in the cell (S) to synthesize AAI. We assume the substrates are found in abundance within the cell at all times, so they do not limit the rate of production of AAI. TraRdim also regulates the production of *traR* by activating the *msh* operon, a suboperon of the *occ* operon containing *traR*. These two positive feedback loops are controlled by the negative regulation of TraRdim by TraM. Transcription of the *traM* mRNA is activated by the dimer itself to produce TraM. This protein essentially blocks TraRdim from binding DNA by forming a stable

complex with the dimer. TraRdim cannot dissociate from TraM and eventually the complex is degraded.

Goryachev et al. assumed the amount of AAI found outside the cell remained constant (2005). However, we know AAI can diffuse in and out of the space around the bacteria, thus entering and leaving the system at will. This was modeled by a rate law:

$$\text{Rate Law for AAI Supply} = \text{AAI Turnover Rate} \times \text{AAI Influx Rate}$$

In this rate law, the amount of autoinducer outside the cell is being replaced at a given rate and there is a steady influx of AAI from outside the system. We also incorporated the degradation of the AAI both inside and outside the cell because we believe this may affect the overall behavior. Our model also included a second cell to examine the effects an additional *Agrobacterium* may have on the system. Therefore, we included a “cell exchange” rate that determined how many molecules of AAI were transferred from one cell to the other in a second. I was interested in manipulating the cell exchange rate and turnover rate to see how the cells reacted in a stochastic model by examining the probability of the system turning “on”.

COPASI

Using a computer software program, we were able to model the rates of various biochemical reactions within the quorum sensing network of *A. tumefaciens*. COPASI is a program specifically designed to model biological systems. Each “Species” of the model was given a name and reactions were set up to relate the species to create the entire quorum sensing model. For instance, the reaction of the importer protein (Imp) binding the “external” autoinducer (Ae) is set up as follows:

$\text{Imp} + \text{Ae} \rightarrow \text{Imp_Ae}$. In this “Reaction” there are three “Species”: Imp, Ae, and Imp_Ae. The rate of reaction is k_4 as described in Table 1. COPASI is able to take these reactions and create a set of differential equations for each species. This set of differential equations can then be run over a set amount of time as a “Time Course”. The time course can be deterministic, stochastic, or a hybrid of the two. At first we observed the characteristic differences between a deterministic model and a stochastic one using the variable of interest – TraRdim. The model was run using 10-second time interval steps for a total of 10,000 seconds (approximately 3 hours). COPASI automatically updates the model every time step with a probability for the next time step based on the rates given in order to create a “Stochastic (Gibson + Bruck)” model. If COPASI is set to “Deterministic”, it simply creates a graph based on the differential equations produced by the various biochemical reactions.

After initial observation, we included the addition of a second cell to the system, which interacted, with the first cell by means of a cell exchange rate. The second cell was entirely identical to the first cell, and thus included the same rates of transcription, translation, and degradation (Table 1). For this model, it was run as “Stochastic (Gibson + Bruck)” for 10,000 seconds with 10-second time interval steps. We manipulated the “cell exchange” and “turnover” rates to observe the interaction between the two cells, as well as the role outside AAI may have on the system. Again, we were interested in the effect these variables had on the population of the dimer – TraRdim. Cell exchange rate was manipulated within the range of 1 to 3 molecules per second, whereas turnover rate was within the range of 0.01 to 0.05 molecules per second to give a coordinate system between these two

variables. These ranges were chosen because of their ability to show large changes in the model in these short ranges, thus giving us more information about the system and specifically these variables. Cells were described as “synchronized” if they were both “on” or both “off” during this time period. Every time a variable was manipulated within the set range, the model was run ten times to count the amount of times cells synchronized in those ten trials. The ‘probability of synchronization’ was determined by dividing the number of times synchronization occurred by ten and multiplying by 100%. A cell was considered “on” in the 10,000 seconds if it reached above 100 particles of the dimer, TraRdim, in that time. This level of dimer was considered to be “on” by Goryachev et al., 2005. The probability of the system turning “on” was determined by the percentage of times the two cells turned “on” in twenty trials at a given coordinate point. So if both cells turned “on” in a single trial then two tallies were marked, if one cell turned “on” only one tally was marked, and if no cells turned “on” then no tallies were marked. The same ten trials were used to measure this value, but since two cells were examined for each run there were twenty total possible trials that may be “on”. To calculate ‘probability “on”’ the number of tallies was divided by twenty and then multiplied by 100% for each variable coordinate. Once trials began the model would not be adjusted until all ten trials were tallied. Every run of the model was marked without ever starting over or negating a trial as to give unbiased results. All other rates were kept constant at the rates described in Goryachev et al., 2005 and in Table 1. An additional rate that related the flux of autoinducer outside the cell, Ae_Supply, was kept at a constant rate of 600 molecules per second. This value was consistent with the “bistable”

region noted by Goryachev et al., 2005. He had shown this region of interest to be around 40-60 nM or 480 to 720 particles of external AAI.

Works Cited

- Al Hajjar, S., & McIntosh, K. (2010). The first influenza pandemic of the 21st century. *Annals of Saudi Medicine*, 30(1), 1–10. doi:10.4103/0256-4947.59365
- Bassler B. L. (1999). How bacteria talk to each other: regulation of gene expression by quorum sensing. *Curr. Opin. Microbiol.* 2, 582–587. 10.1016/S1369-5274(99)00025-9
- Ellner, S., & Guckenheimer, J. (2006). *Dynamic Models in Biology*. Princeton, New Jersey: Princeton University Press.
- Fischer, H. P. (2008). Mathematical Modeling of Complex Biological Systems: From Parts Lists to Understanding Systems Behavior. *Alcohol Research & Health*, 31(1), 49–59.
- Falcao J., Sharp F., Sperandio V. (2004). Cell-to-cell signaling in intestinal pathogens. *Curr Issues Intest Microbiol.* 2004;5:9–17.
- Gentry, S. N., & Jackson, T. L. (2013). A Mathematical Model of Cancer Stem Cell Driven Tumor Initiation: Implications of Niche Size and Loss of Homeostatic Regulatory Mechanisms. *PLoS ONE*, 8(8), e71128. doi:10.1371/journal.pone.0071128
- Gohlke, J., & Deeken, R. (2014). Plant responses to *Agrobacterium tumefaciens* and crown gall development. *Frontiers in Plant Science*, 5, 155. doi:10.3389/fpls.2014.00155

- Goryachev A. B. (2009). Design principles of the bacterial quorum sensing gene networks. *Wiley Interdiscip. Rev. Syst. Biol. Med.* 1, 45–60 10.1002/wsbm.27
- Goryachev A.B., Toh D.J., Lee T. (2005). Systems analysis of a quorum sensing network: design constraints imposed by the functional requirements, network topology and kinetic constants. *Biosystems.* 2005;83:178–187.
- Goryachev A. B., Toh D. J., Wee K. B., Lee T., Zhang H. B., Zhang L. H. (2005). Transition to quorum sensing in an *Agrobacterium* population: a stochastic model. *PLoS Comput. Biol.* 1:e3710.1371/journal.pcbi.0010037
- Haruta, S., Yoshida, T., Aoi, Y., Kaneko, K., & Futamata, H. (2013). Challenges for Complex Microbial Ecosystems: Combination of Experimental Approaches with Mathematical Modeling. *Microbes and Environments*, 28(3), 285–294. doi:10.1264/jsme2.ME13034
- Haudecoeur E, Faure D. (2010). A fine control of quorum-sensing communication in *Agrobacterium tumefaciens*. *Commun Integr Biol.* 2010;3:84–88.
- Jasuja N., Sehgal P. (2015). "Gram-negative Bacteria vs Gram-positive Bacteria." *Diffen.com*. Diffen LLC, n.d. Web. 10 Jan 2015.
- Jones, B., & Nishiguchi, M. (2004). Counterillumination in the Hawaiian bobtail squid, *Euprymna scolopes* Berry (Mollusca: Cephalopoda). *Marine Biology*, 144(6), 1151-1155.
- Miller M. B., Bassler B. L. (2001). Quorum sensing in bacteria. *Annual Review of Microbiology.* 2001;55:165–199. doi: 10.1146/annurev.micro.55.1.165.
- Nealson K. H., Hastings J. W. (1979). Bacterial bioluminescence: its control and ecological significance. *Microbiol. Rev.* 43, 496–518.

- Parham, P. (2015). *The Immune System* (4th ed.). New York, NY: Garland Science.
- Reading N. C., Sperandio V. (2006). Quorum sensing: the many languages of bacteria. *FEMS Microbiol. Lett.* 254, 1–11.10.1111/j.1574-6968.2005.00001.x
- Rutherford ST, Bassler BL (2012) Bacterial quorum sensing: its role in virulence and possibilities for its control. *Cold Spring Harb Perspect Med* 2.
- Salton MRJ, Kim KS. Structure. In: Baron S, editor. *Medical Microbiology*. 4th edition. Galveston (TX): University of Texas Medical Branch at Galveston; 1996. Chapter 2. Available from: <http://www.ncbi.nlm.nih.gov/books/NBK8477/>
- Sauvage E., Kerff F., Terrak M., Ayala J.A., Charlier P. (2008). The penicillin-binding proteins: structure and role in peptidoglycan biosynthesis. *FEMS Microbiol Rev* 32:234–258.
- Schaechter, M., Ingraham, J., & Neidhardt, F. (2006). *Microbe*. Washington, D.C.: American Society for Microbiology.
- Subramoni, S., Nathoo, N., Klimov, E., & Yuan, Z.-C. (2014). *Agrobacterium tumefaciens* responses to plant-derived signaling molecules. *Frontiers in Plant Science*, 5, 322. doi:10.3389/fpls.2014.00322
- Weber M., Buceta J. (2013). Dynamics of the quorum sensing switch: stochastic and non-stationary effects. *BMC Syst. Biol.* 7:6.10.1186/1752-0509-7-6
- Wilkinson, D. (2012). *Stochastic Modelling for Systems Biology* (2nd ed.). Boca Raton, Florida: Taylor & Francis Group, LLC.
- Wilson, B., Salyers, A., Whitt, D., & Winkler, M. (2011). *Bacterial Pathogenesis: A Molecular Approach* (3rd ed.). Washington, D.C.: ASM Press.

Acknowledgements

I would like to thank David Brown of the Mathematics Department at Colorado College for his expertise in mathematical biology and interest in quorum sensing research that allowed me to work alongside him to produce these results, as well as his constructive criticism while finalizing this thesis. I would also like to thank Phoebe Lostroh in the Molecular Biology Department of Colorado College for her expertise in molecular biology to critique my research as a second reader. Thanks also to the Dean's Office of Colorado College for their funding of this research via the faculty-student collaborative research grant.

Tables

Table 1. Rates of biochemical reactions in the quorum sensing network of *Agrobacterium tumefaciens*. Biochemical rate laws are as written in COPASI and are for both cells. Values are estimates given by Goryachev et al., 2005. Items in red were manipulated for evaluation of the two-cell model.

Rate Constant	Value	Action	Biochemical Rate Law
k1	0.3 s^{-1}	Production of AAI by TraI (Cell 1)	$\text{TraI}\{\text{"Cell 1"}\} \rightarrow \text{TraI}\{\text{"Cell 1"}\} + \text{Ai}\{\text{"Cell 1"}\}$
k1	0.3 s^{-1}	Production of AAI by TraI (Cell 2)	$\text{TraI}\{\text{"Cell 2"}\} \rightarrow \text{TraI}\{\text{"Cell 2"}\} + \text{Ai}\{\text{"Cell 2"}\}$
k2	0.14 s^{-1}	Passive Diffusion of AAI Into the Cell	$\text{Ae}\{\text{"Cell 1"}\} \rightarrow \text{Ai}\{\text{"Cell 1"}\}$
k2	0.14 s^{-1}	Passive Diffusion of AAI Into the Cell	$\text{Ae}\{\text{"Cell 2"}\} \rightarrow \text{Ai}\{\text{"Cell 2"}\}$
k2	0.14 s^{-1}	Passive Diffusion of AAI Out the Cell	$\text{Ai}\{\text{"Cell 1"}\} \rightarrow \text{Ae}\{\text{"Cell 1"}\}$
k2	0.14 s^{-1}	Passive Diffusion of AAI Out the Cell	$\text{Ai}\{\text{"Cell 2"}\} \rightarrow \text{Ae}\{\text{"Cell 2"}\}$
k3	0.4 s^{-1}	Active Transport of AAI by Imp (Cell 1)	$\text{Imp_Ae}\{\text{"Cell 1"}\} \rightarrow \text{Ai}\{\text{"Cell 1"}\} + \text{Imp}\{\text{"Cell 1"}\}$
k3	0.4 s^{-1}	Active Transport of AAI by Imp (Cell 2)	$\text{Imp_Ae}\{\text{"Cell 2"}\} \rightarrow \text{Ai}\{\text{"Cell 2"}\} + \text{Imp}\{\text{"Cell 2"}\}$
k4	$0.04 \text{ m}^{-1} \cdot \text{s}^{-1}$	Imp Binding AAI (Cell 1)	$\text{Imp}\{\text{"Cell 1"}\} + \text{Ae}\{\text{"Cell 1"}\} \rightarrow \text{Imp_Ae}\{\text{"Cell 1"}\}$
k4	$0.04 \text{ m}^{-1} \cdot \text{s}^{-1}$	Imp Binding AAI (Cell 2)	$\text{Imp}\{\text{"Cell 2"}\} + \text{Ae}\{\text{"Cell 2"}\} \rightarrow \text{Imp_Ae}\{\text{"Cell 2"}\}$
k5	$2 \cdot 10^{-3} \text{ s}^{-1}$	Imp Dissociating AAI (Cell 1)	$\text{Imp_Ae}\{\text{"Cell 1"}\} \rightarrow \text{Imp}\{\text{"Cell 1"}\} + \text{Ae}\{\text{"Cell 1"}\}$
k5	$2 \cdot 10^{-3} \text{ s}^{-1}$	Imp Dissociating AAI (Cell 2)	$\text{Imp_Ae}\{\text{"Cell 2"}\} \rightarrow \text{Imp}\{\text{"Cell 2"}\} + \text{Ae}\{\text{"Cell 2"}\}$
k6	$3.56 \cdot 10^{-5} \text{ m}^{-1} \cdot \text{s}^{-1}$	Formation of TraR Complex with AAI	$\text{imptrar}\{\text{"Cell 1"}\} + \text{Ai}\{\text{"Cell 1"}\} \rightarrow \text{TraR}\{\text{"Cell 1"}\} + \text{imptrar}\{\text{"Cell 1"}\}$
k6	$3.56 \cdot 10^{-5} \text{ m}^{-1} \cdot \text{s}^{-1}$	Formation of TraR Complex with AAI	$\text{imptrar}\{\text{"Cell 2"}\} + \text{Ai}\{\text{"Cell 2"}\} \rightarrow \text{TraR}\{\text{"Cell 2"}\} + \text{imptrar}\{\text{"Cell 2"}\}$
k7	$1.5 \cdot 10^{-2} \text{ m} \cdot \text{s}^{-1}$	Transcription rate of the occ Operon	$\rightarrow \text{imptrar}\{\text{"Cell 1"}\}$
k7	$1.5 \cdot 10^{-2} \text{ m} \cdot \text{s}^{-1}$	Transcription rate of the occ Operon	$\rightarrow \text{imptrar}\{\text{"Cell 2"}\}$

k8	$1.0 \cdot 10^{-3} \text{ m}^{-1} \cdot \text{s}^{-1}$	Dimerization of TraR (Cell 1)	$2 * \text{TraR}\{\text{"Cell 1"}\} \rightarrow \text{TraRd}\{\text{"Cell 1"}\}$
k8	$1.0 \cdot 10^{-3} \text{ m}^{-1} \cdot \text{s}^{-1}$	Dimerization of TraR (Cell 2)	$2 * \text{TraR}\{\text{"Cell 2"}\} \rightarrow \text{TraRd}\{\text{"Cell 2"}\}$
k9	$1 \cdot 10^{-4} \text{ s}^{-1}$	Dissociation of TraRd Dimer (Cell 1)	$\text{TraRd}\{\text{"Cell 1"}\} \rightarrow 2 * \text{TraR}\{\text{"Cell 1"}\}$
k9	$1 \cdot 10^{-4} \text{ s}^{-1}$	Dissociation of TraRd Dimer (Cell 2)	$\text{TraRd}\{\text{"Cell 2"}\} \rightarrow 2 * \text{TraR}\{\text{"Cell 2"}\}$
k10	$3.3 \cdot 10^{-4} \text{ s}^{-1}$	Degradation of TraRd (Cell 1)	$\text{TraRd}\{\text{"Cell 1"}\} \rightarrow$
k10	$3.3 \cdot 10^{-4} \text{ s}^{-1}$	Degradation of TraRd (Cell 2)	$\text{TraRd}\{\text{"Cell 2"}\} \rightarrow$
k11	$8.3 \cdot 10^{-4} \text{ m}^{-1} \cdot \text{s}^{-1}$	Formation of TraRd Complex with TraM	$\text{TraRd}\{\text{"Cell 1"}\} + \text{TraM}\{\text{"Cell 1"}\} \rightarrow$
k11	$8.3 \cdot 10^{-4} \text{ m}^{-1} \cdot \text{s}^{-1}$	Formation of TraRd Complex with TraM	$\text{TraRd}\{\text{"Cell 2"}\} + \text{TraM}\{\text{"Cell 2"}\} \rightarrow$
k12	$6 \cdot 10^{-3} \text{ s}^{-1}$	Degradation of msh mRNA (Cell 1)	$\text{imptrar}\{\text{"Cell 1"}\} \rightarrow$
k12	$6 \cdot 10^{-3} \text{ s}^{-1}$	Degradation of msh mRNA (Cell 2)	$\text{imptrar}\{\text{"Cell 2"}\} \rightarrow$
k13	$1.6 \cdot 10^{-2} \text{ s}^{-1}$	Translation of msh mRNA (Cell 1)	$\text{imptrar}\{\text{"Cell 1"}\} \rightarrow \text{imptrar}\{\text{"Cell 1"}\} + \text{Imp}\{\text{"Cell 1"}\}$
k13	$1.6 \cdot 10^{-2} \text{ s}^{-1}$	Translation of msh mRNA (Cell 2)	$\text{imptrar}\{\text{"Cell 2"}\} \rightarrow \text{imptrar}\{\text{"Cell 2"}\} + \text{Imp}\{\text{"Cell 2"}\}$
k14	$1.0 \cdot 10^{-4} \text{ s}^{-1}$	Degradation of Imp (Cell 1)	$\text{Imp}\{\text{"Cell 1"}\} \rightarrow$
k14	$1.0 \cdot 10^{-4} \text{ s}^{-1}$	Degradation of Imp (Cell 2)	$\text{Imp}\{\text{"Cell 2"}\} \rightarrow$
k15	$1.6 \cdot 10^{-2} \text{ m} \cdot \text{s}^{-1}$	Transcription of traM (Cell 1)	$\text{TraRd_tram}\{\text{"Cell 1"}\} \rightarrow \text{traM}\{\text{"Cell 1"}\} + \text{TraRd_tram}\{\text{"Cell 1"}\}$
k15	$1.6 \cdot 10^{-2} \text{ m} \cdot \text{s}^{-1}$	Transcription of traM (Cell 2)	$\text{TraRd_tram}\{\text{"Cell 2"}\} \rightarrow \text{traM}\{\text{"Cell 2"}\} + \text{TraRd_tram}\{\text{"Cell 2"}\}$
k16	$1.4 \cdot 10^{-2} \text{ m}^{-1} \cdot \text{s}^{-1}$	TraRd Binding tram (Cell 1)	$\text{TraRd}\{\text{"Cell 1"}\} + \text{tram}\{\text{"Cell 1"}\} \rightarrow \text{TraRd_tram}\{\text{"Cell 1"}\}$
k16	$1.4 \cdot 10^{-2} \text{ m}^{-1} \cdot \text{s}^{-1}$	TraRd Binding tram (Cell 2)	$\text{TraRd}\{\text{"Cell 2"}\} + \text{tram}\{\text{"Cell 2"}\} \rightarrow \text{TraRd_tram}\{\text{"Cell 2"}\}$
k17	$9.26 \cdot 10^{-3} \text{ s}^{-1}$	TraRd Dissociating tram (Cell 1)	$\text{TraRd_tram}\{\text{"Cell 1"}\} \rightarrow \text{TraRd}\{\text{"Cell 1"}\} + \text{tram}\{\text{"Cell 1"}\}$

k17	$9.26 \cdot 10^{-3} \text{ s}^{-1}$	TraRd Dissociating tram (Cell 2)	TraRd_tram{"Cell 2"} -> TraRd{"Cell 2"} + tram{"Cell 2"}
k18	$1.6 \cdot 10^{-3} \text{ s}^{-1}$	Degradation of traM mRNA (Cell 1)	traM{"Cell 1"} ->
k18	$1.6 \cdot 10^{-3} \text{ s}^{-1}$	Degradation of traM mRNA (Cell 2)	traM{"Cell 2"} ->
k19	$1.92 \cdot 10^{-2} \text{ s}^{-1}$	Translation of traM mRNA (Cell 1)	traM{"Cell 1"} -> traM{"Cell 1"} + TraM{"Cell 1"}
k19	$1.92 \cdot 10^{-2} \text{ s}^{-1}$	Translation of traM mRNA (Cell 2)	traM{"Cell 2"} -> traM{"Cell 2"} + TraM{"Cell 2"}
k20	$8 \cdot 10^{-5} \text{ s}^{-1}$	TraM Degradation (Cell 1)	TraM{"Cell 1"} ->
k20	$8 \cdot 10^{-5} \text{ s}^{-1}$	TraM Degradation (Cell 2)	TraM{"Cell 2"} ->
k21	$1.6 \cdot 10^{-2} \text{ m} \cdot \text{s}^{-1}$	Transcription of trb Operon (Cell 1)	TraRd_trb{"Cell 1"} -> tral{"Cell 1"}
k21	$1.6 \cdot 10^{-2} \text{ m} \cdot \text{s}^{-1}$	Transcription of trb Operon (Cell 2)	TraRd_trb{"Cell 2"} -> tral{"Cell 2"}
k22	$2.68 \cdot 10^{-2} \text{ m}^{-1} \cdot \text{s}^{-1}$	TraRd Binding trb (Cell 1)	TraRd{"Cell 1"} + trb{"Cell 1"} -> TraRd_trb{"Cell 1"}
k22	$2.68 \cdot 10^{-2} \text{ m}^{-1} \cdot \text{s}^{-1}$	TraRd Binding trb (Cell 2)	TraRd{"Cell 2"} + trb{"Cell 2"} -> TraRd_trb{"Cell 2"}
k23	$2.2 \cdot 10^{-2} \text{ s}^{-1}$	TraRd Dissociating trb (Cell 1)	TraRd_trb{"Cell 1"} -> TraRd{"Cell 1"} + trb{"Cell 1"}
k23	$2.2 \cdot 10^{-2} \text{ s}^{-1}$	TraRd Dissociating trb (Cell 2)	TraRd_trb{"Cell 2"} -> TraRd{"Cell 2"} + trb{"Cell 2"}
k24	$6.0 \cdot 10^{-3} \text{ s}^{-1}$	Degradation of tral mRNA (Cell 1)	tral{"Cell 1"} ->
k24	$6.0 \cdot 10^{-3} \text{ s}^{-1}$	Degradation of tral mRNA (Cell 2)	tral{"Cell 2"} ->
k25	$1.6 \cdot 10^{-2} \text{ s}^{-1}$	Translation of tral mRNA (Cell 1)	tral{"Cell 1"} -> tral{"Cell 1"} + Tral{"Cell 1"}
k25	$1.6 \cdot 10^{-2} \text{ s}^{-1}$	Translation of tral mRNA (Cell 2)	tral{"Cell 2"} -> tral{"Cell 2"} + Tral{"Cell 2"}
k26	$1.0 \cdot 10^{-4} \text{ s}^{-1}$	Tral Degradation (Cell 1)	Tral{"Cell 1"} ->
k26	$1.0 \cdot 10^{-4} \text{ s}^{-1}$	Tral Degradation (Cell 2)	Tral{"Cell 2"} ->

k27	$2.3 \cdot 10^{-4} \text{ m} \cdot \text{s}^{-1}$	tral Constitutive Expression (Cell 1)	-> tral{"Cell 1"}
k27	$2.3 \cdot 10^{-4} \text{ m} \cdot \text{s}^{-1}$	tral Constitutive Expression (Cell 2)	-> tral{"Cell 2"}
k28	$2.2 \cdot 10^{-2} \text{ m} \cdot \text{s}^{-1}$	Transcription of msh Operon (Cell 1)	TraRd_msh{"Cell 1"} -> imprar{"Cell 1"} + TraRd_msh{"Cell 1"}
k28	$2.2 \cdot 10^{-2} \text{ m} \cdot \text{s}^{-1}$	Transcription of msh Operon (Cell 2)	TraRd_msh{"Cell 2"} -> imprar{"Cell 2"} + TraRd_msh{"Cell 2"}
k29	$2.9 \cdot 10^{-3} \text{ m}^{-1} \cdot \text{s}^{-1}$	TraRd Binding msh (Cell 1)	TraRd{"Cell 1"} + msh{"Cell 1"} -> TraRd_msh{"Cell 1"}
k29	$2.9 \cdot 10^{-3} \text{ m}^{-1} \cdot \text{s}^{-1}$	TraRd Binding msh (Cell 2)	TraRd{"Cell 2"} + msh{"Cell 2"} -> TraRd_msh{"Cell 2"}
k30	$2.4 \cdot 10^{-3} \text{ s}^{-1}$	TraRd Dissociating msh (Cell 1)	TraRd_msh{"Cell 1"} -> TraRd{"Cell 1"} + msh{"Cell 1"}
k30	$2.4 \cdot 10^{-3} \text{ s}^{-1}$	TraRd Dissociating msh (Cell 2)	TraRd_msh{"Cell 2"} -> TraRd{"Cell 2"} + msh{"Cell 2"}
k31	$6.418 \cdot 10^{-4} \text{ s}^{-1}$	Degradation of AAI Outside of Cell (Cell 1)	Ae{"Cell 1"} ->
k31	$6.418 \cdot 10^{-4} \text{ s}^{-1}$	Degradation of AAI Outside of Cell (Cell 2)	Ae{"Cell 2"} ->
k31	$6.418 \cdot 10^{-4} \text{ s}^{-1}$	Degradation of AAI Inside of Cell (Cell 1)	Ai{"Cell 1"} ->
k31	$6.418 \cdot 10^{-4} \text{ s}^{-1}$	Degradation of AAI Inside of Cell (Cell 2)	Ai{"Cell 2"} ->
Turnover	$0.01 - 0.05 \text{ s}^{-1}$	Diffusion of AAI Out of System (Cell 2)	Ae{"Cell 1"} ->
Turnover	$0.01 - 0.05 \text{ s}^{-1}$	Diffusion of AAI Out of System (Cell 2)	Ae{"Cell 2"} ->
Rate Law	Turnover*600 s^{-1}	Supply of AAI From Environment (Cell 1)	-> Ae{"Cell 1"}
Rate Law	Turnover*600 s^{-1}	Supply of AAI From Environment (Cell 2)	-> Ae{"Cell 2"}
Cell Exchange	$1-3 \text{ s}^{-1}$	Diffusion From Cell 1 to Cell 2	Ae{"Cell 1"} -> Ae{"Cell 2"}
Cell Exchange	$1-3 \text{ s}^{-1}$	Diffusion From Cell 2 to Cell 1	Ae{"Cell 2"} -> Ae{"Cell 1"}

Figures

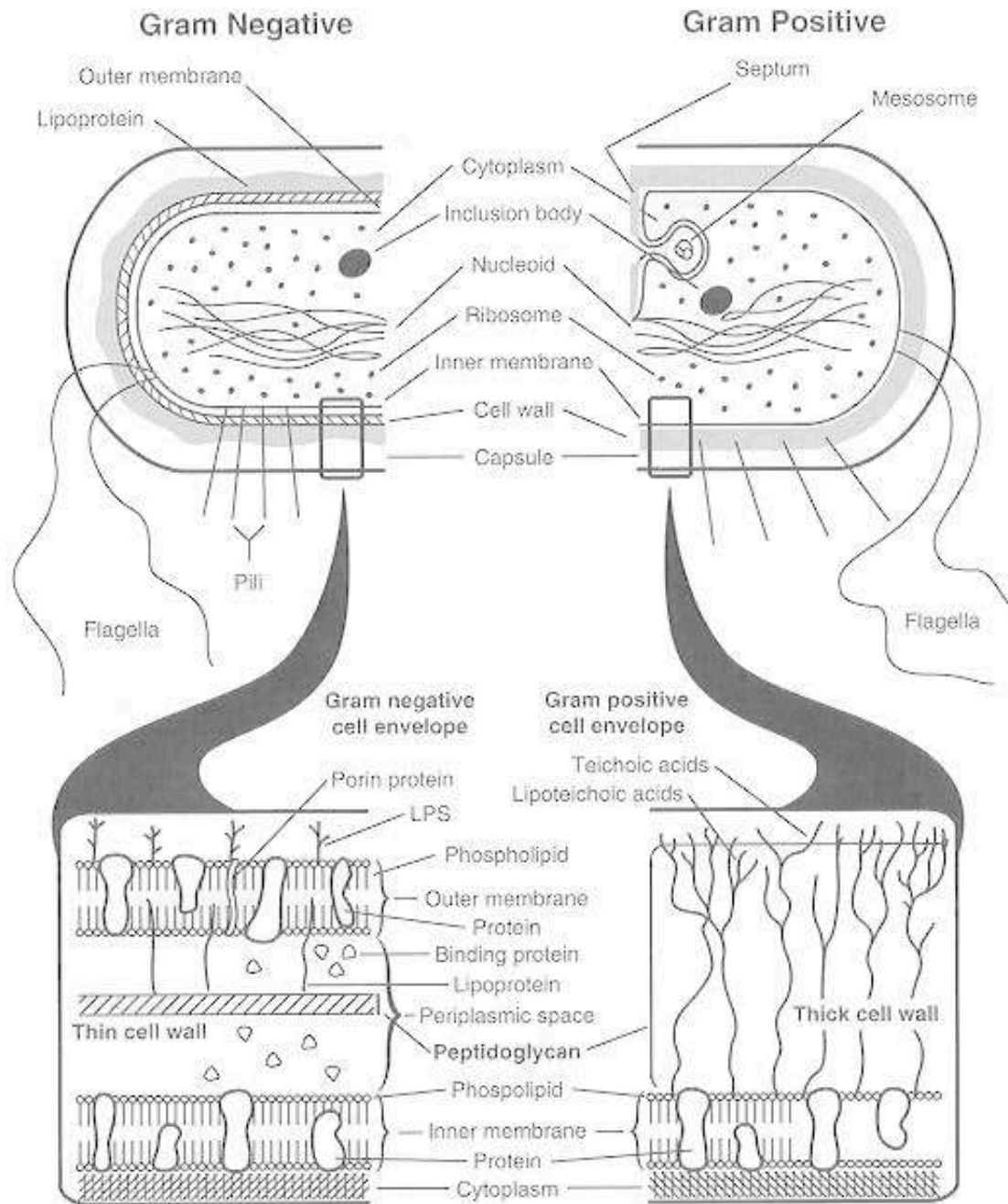


Fig 1. The comparison of gram-negative and gram-positive bacteria. Adopted from Medical Microbiology, 4th Edition. (1996).

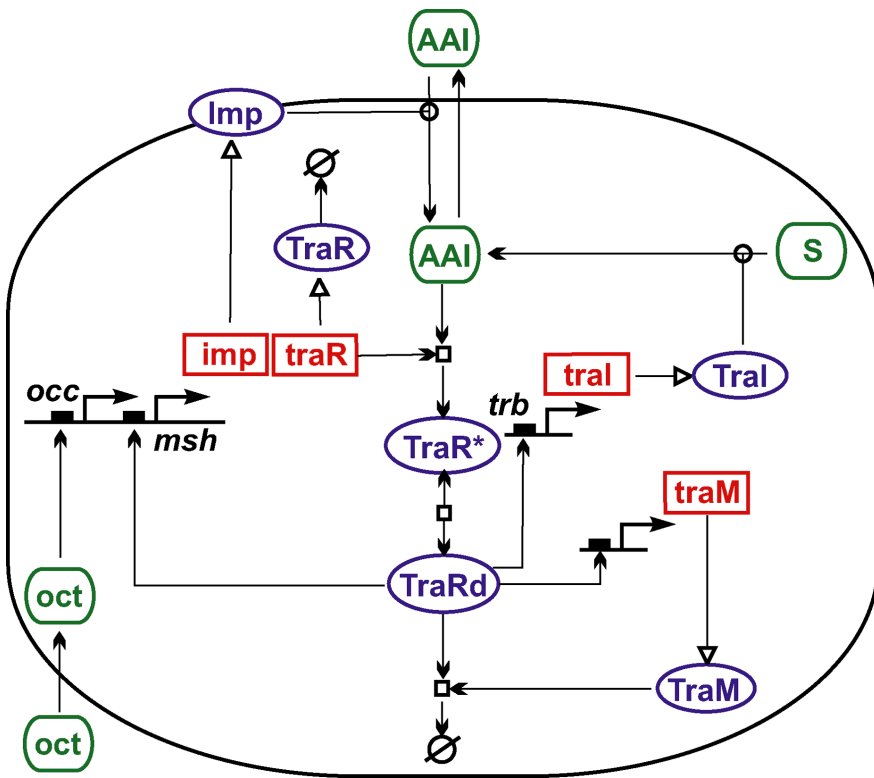


Fig 2. Complex model of the quorum sensing network in *Agrobacterium tumefaciens*. Adopted from Goryachev et al., 2005.

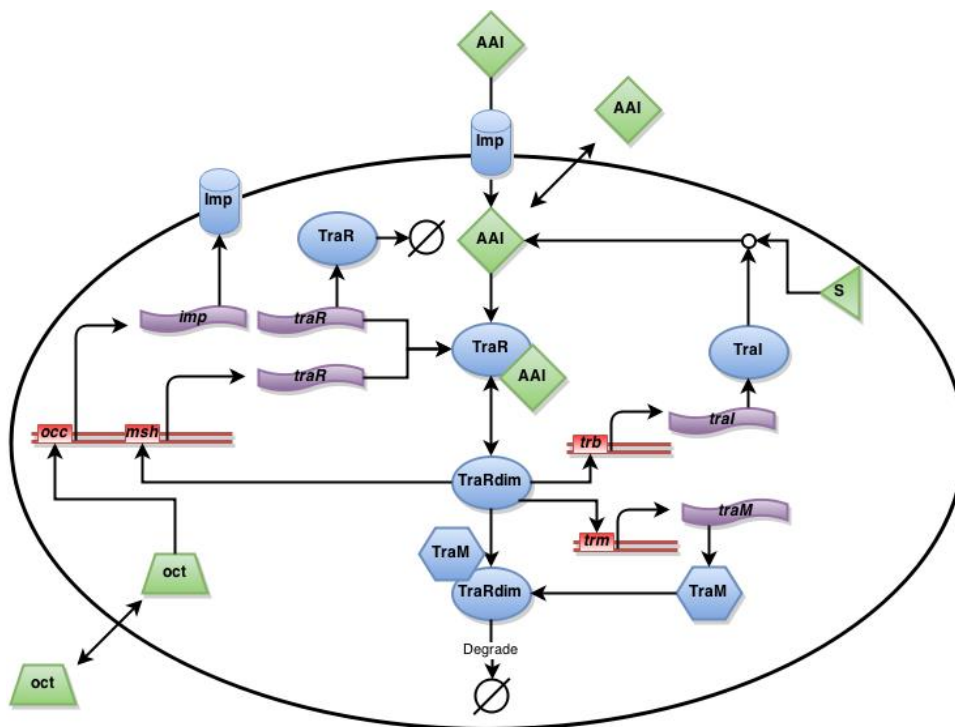


Fig 3. Single-cell model of the quorum sensing network in *Agrobacterium tumefaciens*. This model is adopted from Goryachev et al., 2005.

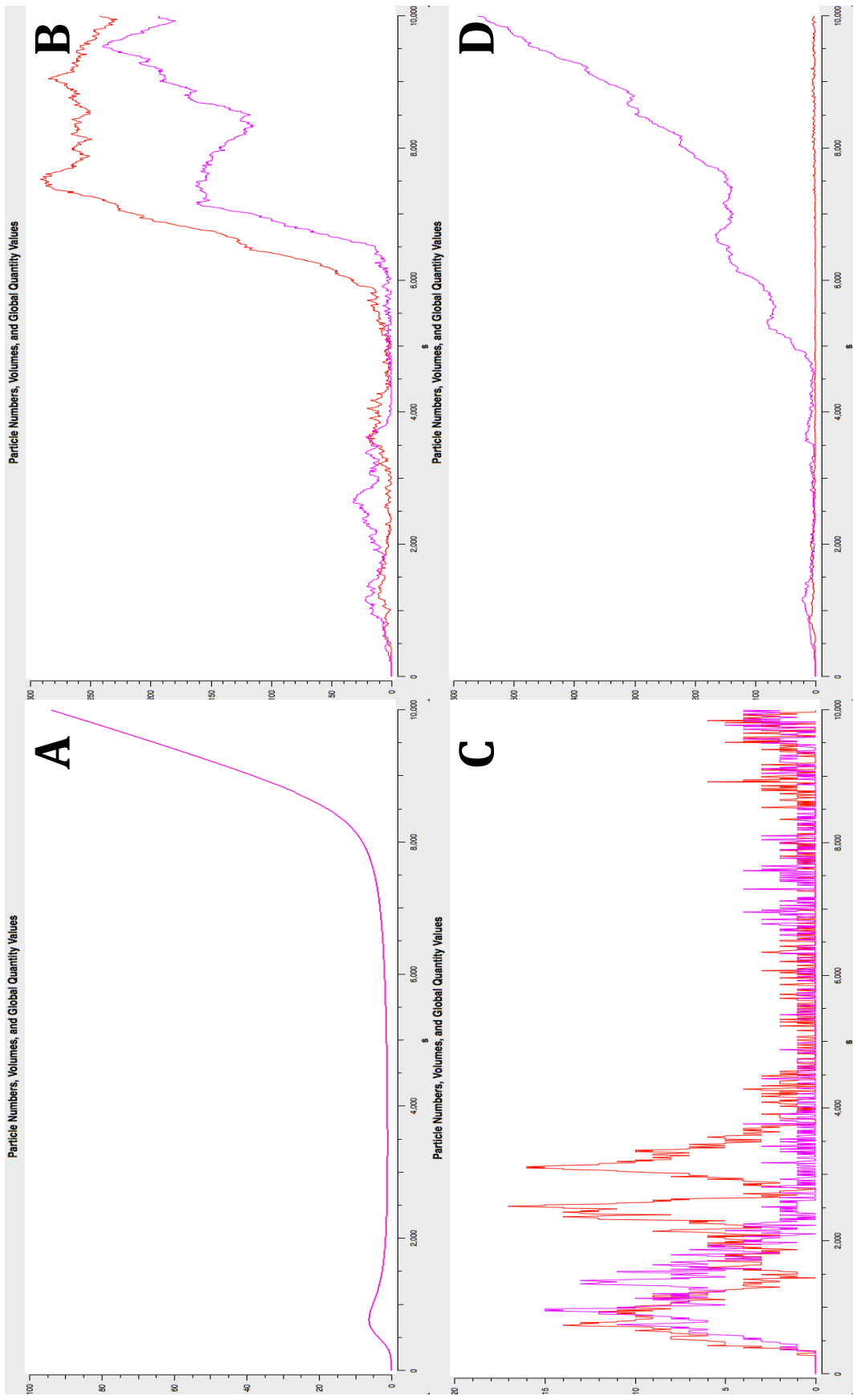


Fig 4. Time course runs of the quorum sensing model using COPASI show differences between deterministic and stochastic. All runs use a cell exchange rate of 3 and a turnover rate of 0.03. The variable of interest is TraRdim shown in purple for cell 1 and red for cell 2. **A.** shows a deterministic run of the model. **B.** shows both cells synchronized turning “on”. **C.** is both cells synchronized staying “off”. **D.** shows two cells independent of each other – cell 1 turns “on” and cell 2 is remains “off”.

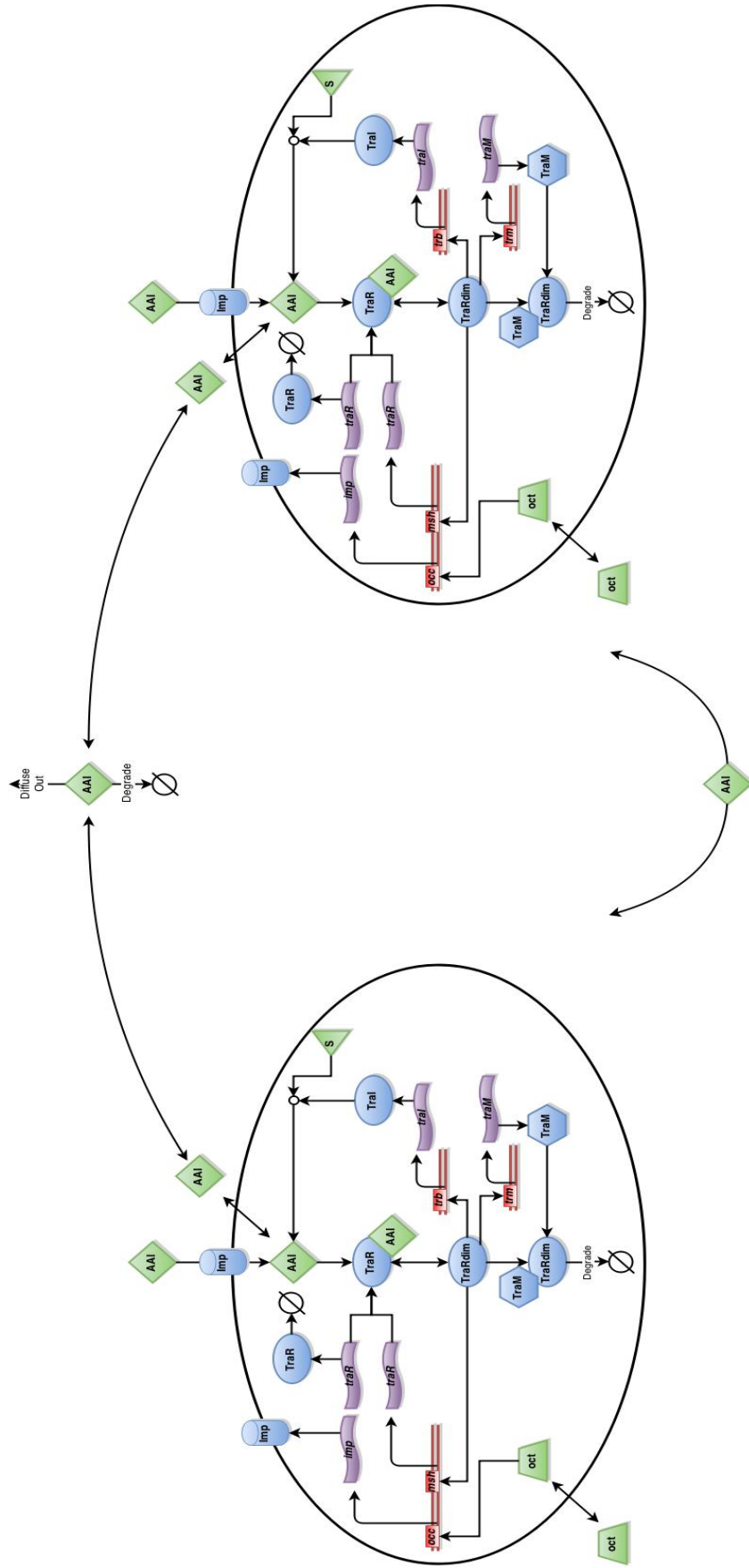


Fig 5. Two-cell model of quorum sensing network in *Agrobacterium tumefaciens*. Cells communicate through an autoinducer (AAI) at a cell exchange rate. The autoinducer is also removed from the system via degradation or diffusion and can also be added via an influx.

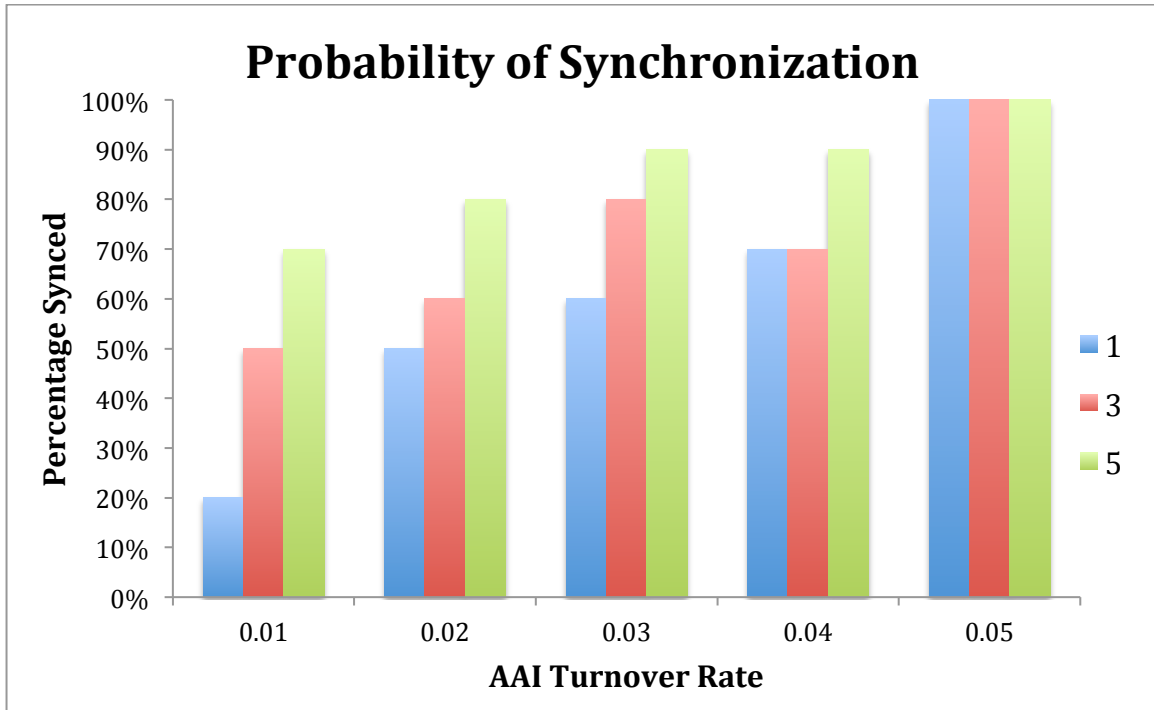


Fig 6. Results of the two-cell model. The probability of cells synchronizing is given by the amount of times the cells acted similar (both “on” or both “off”) in ten trials.

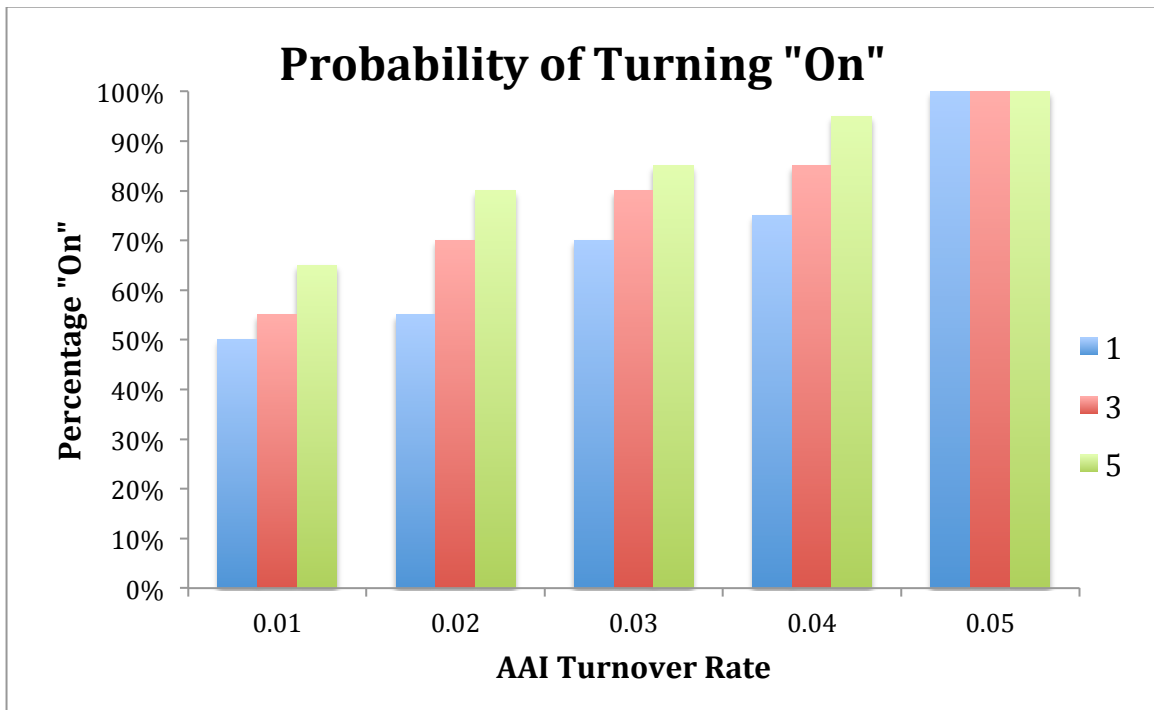


Fig 7. Results of the two-cell model. The probability of a cell turning “on” is given by the average of the amount of times a cell turned “on” for twenty total trials.